2004 International Symposium on Nonlinear
Theory and its Applications (NOLTA2004)
Fukuoka, Japan, Nov. 29 - Dec. 3, 2004

Neuronal Chaos with Very Long Inter-Spike Intervals near the Hopf Bifurcation of an Equilibrium Point

Shinji Doi† and Sadatoshi Kumagai

Department of Electrical Engineering, Graduate School of Engineering, Osaka University,
2-1 Yamada-oka, Suita, 565-0871, Japan
†Email: doi@pwr.eng.osaka-u.ac.jp

Abstract—Using the three-dimensional Bonhoeffer-van der Pol equations, it is shown that chaotic and extraordinarily slow oscillations appear near a Hopf bifurcation point of an equilibrium point. Using the so-called slow-fast decomposition analysis of singularly perturbed dynamical systems, the generation mechanism of chaotic and slow oscillations is explored. In particular, the phenomenology of birth of the slow oscillations can become different according as the bifurcation of a subsystem is Hopf or saddle-node.

1. Introduction

Neurons produce a characteristic waveform called spike which is rapid increase and decrease of cell-membrane voltage. Spikes are the main information carrier in nervous systems and thus the analysis of the generation process of spikes and of the inter-spike-intervals (ISIs) are very important. Recently, chaotic spiking and long ISIs (or slow oscillations) in neurons attract much attention [5, 8, 10]. Guckenheimer and Oliva showed the existence of a chaotic solution in the Hodgkin-Huxley (HH) equations of the most famous neuronal model *without any periodic inputs* [9], although the chaotic solution is highly unstable. On the other hand, we have discovered more stable and generic chaotic spiking in the slightly modified HH equations [1, 3]. We have also shown that the chaotic solution frequently accompanies very long ISIs. The striking feature is that the transition from a stable equilibrium point to chaotic and slow spiking is caused by a simple Hopf bifurcation. The precise mechanism of the chaotic and slow spiking, however, has not yet clarified since the HH equations contain many complicated nonlinear functions.

In the present paper, we show that similar chaotic and slow spiking near a Hopf bifurcation can be observed in the three-dimensional Bonhoeffer-van der Pol equations which are much simpler neuronal model than the HH equations. The generation mechanism of the chaotic and slow spiking is explored by the so-called slow-fast decomposition analysis of singularly perturbed dynamical systems. Especially, we show that the phenomenology of the generation of chaotic and slow spiking is much dependent of the type of bifurcation of a fast subsystem.

2. Long ISI in the Extended Bonhoeffer-van der Pol Neuronal Model

Consider the extended Bonhoeffer-van der Pol (BVP) or FitzHugh-Nagumo (FHN) equations [2, 11]:

$$\frac{dx}{dt} = x - x^3/3 - y - z + I_{\text{ext}}, \tag{1a}$$

$$\frac{dy}{dt} = \eta(x - ay), \tag{1b}$$

$$\frac{dz}{dt} = \epsilon(x - bz), \qquad \epsilon \ll 1, \tag{1c}$$

where x corresponds to a membrane potential and y a refractory variable in terms of neuroscience. z is also a refractory or inhibitory variable since the increase of z eventually operates to reduce x (but very slowly owing to $\epsilon \ll 1$). If the variable z is ignored, the equations (1) are the same as the (two-dimensional) original BVP or FHN equations [6]. Although the only extension from the original BVP model is the addition of the linear term z in (1a) and the linear equation (1c), there are much differences in their dynamics: The extended BVP equations with three variables can possess both bursting and chaotic solutions while the original two-dimensional BVP equations have neither. The analysis of such complicated behavior of the extended BVP equations has already been done [2, 11]. In the present paper, however, we focus on the long ISIs near the generation point of repetitive firing or spiking.

Figure 1 shows the inter-spike interval (ISI) as a function of the parameter (external current) I_{ext}. Both axes are denoted in a logarithmic scale and the value of I_{ext} is denoted as the deviation Δ from its value at the Hopf bifurcation point. Between the upper panels (a-i,ii,iii) and the lower panels (b-i,ii,iii), the values of the parameters a, b and η are different (the meaning of this difference will become clearer later). From the left panels (a,b-i) to right panels (a,b-iii), the value of ϵ is decreased.

The ISIs grow up as I_{ext} decreases. Over a wide range of I_{ext} of Fig.1, ISI takes multiple values for each value of the bifurcation parameter I_{ext}; ISI varies spike by spike. This variation is much larger in upper panels than in the lower panels. Near the left part of panel (a-i), the ISI takes large values over one hundred thousands. Since the constant ϵ is just 0.01 and is not so small, the ISI over one-hundred

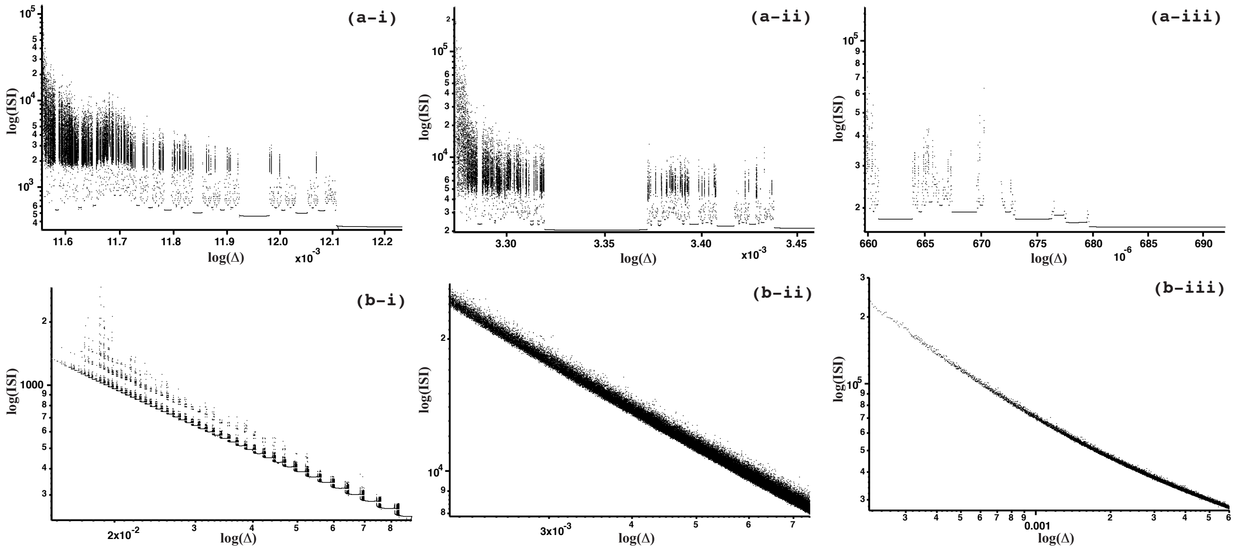

Figure 1: ISI of the BVP equations in a log-log scale. **(a)** $a = 3.0$, $b = 1.0$, $\eta = 0.13$. **(b)** $a = 1.5$, $b = 1.0$, $\eta = 0.1$. The values of ϵ are: **(i)** 0.01, **(ii)** 0.001, **(iii)** 0.0001. Following an initial transient of 10,000 time integration of (1), ISIs are recorded during 500,000 time for each of equally spaced two thousands I_{ext} values on the abscissa. The variable Δ in the abscissa is the deviation of I_{ext} values from the Hopf bifurcation point. The values of I_{ext} where the Hopf bifurcation occurs are: **(a-i)** -0.488734, **(a-ii)** -0.460859, **(a-iii)** -0.454502, **(b-i)** -0.888645, **(b-ii)** -0.877411, **(b-iii)** -0.876014.

thousands is extraordinarily large. Figure 2(a) is an example of the slow spiking shown in Fig.1(a-i). We can see that the ISI varies from a small value as several thousands to a large value as fifty thousands. Also, the sub-threshold oscillation (near $x = -0.85$) is apparently very chaotic; panel (b) is the magnification of the sub-threshold oscillation.

In the panel (b-i) of Fig.1, ISI also grows up as I_{ext} decreases although the ISI growth is not so large as panel (a-i). The ISI value, however, is more than two thousands and is also extraordinarily large since ϵ is just 0.01. Figure 2(c) is an example of slow oscillations with long ISIs shown in Fig.1(b-i). In this case, the solution stays near a resting potential (an unstable equilibrium near $x = -1$) for a long time without sub-threshold oscillation and then the amplitude of sub-threshold oscillation gradually grows up and finally produces a spike. The solution of (c) is considered as a periodic solution differently from the chaotic one of (a).

Note that, in Fig.1, the minimum value of the abscissa becomes smaller as the value of ϵ decreases (from the left panels to right ones). Since Δ is the deviation of I_{ext} from its value at the Hopf bifurcation point, we can see that the generation point of slow spiking approaches the Hopf bifurcation point as ϵ decreases. The maximum ISI values of the upper panels of Fig.1 are much bigger than those of the panels of the lower row, and apparently do not depend on the ϵ value while the maximum ISI values of lower panels do depend on ϵ.

The bifurcation structure of equilibrium points of the BVP equations is very simple one (not shown here); the number of the equilibrium point is unique for all values of the bifurcation parameter I_{ext} (when the values of the other parameters were set as in Fig.1) and the stability of the unique equilibrium point changes through a supercritical Hopf bifurcation. In the HH equations, the Hopf bifurcations were subcritical [1, 3]. Thus, the slow and chaotic oscillations near a Hopf bifurcation point shown in the present paper do not depend on the type of Hopf bifurcation and are considered to be very generic ones. In the case of the upper panels of Fig.1, periodic orbits with small amplitudes bifurcated from the Hopf bifurcation suffer a period-doubling bifurcation and an additional cascade of period-doubling bifurcations occurs. In the case of the lower panels of Fig.1, all Hopf bifurcations are also supercritical and the periodic orbits bifurcated at the Hopf bifurcation suffer a torus bifurcation. Slow spiking exists after the torus bifurcation (bigger values of I_{ext}). Thus, we expect that some of the ISI variations shown in the lower panels of Fig.1 correspond to the quasi-periodic behavior rather than the chaotic one of the upper panels.

3. Slow-Fast Decomposition Analysis

In order to clarify the mechanism of the very slow spiking, we make a so-called slow-fast decomposition analysis [7] in the followings. A system with multiple time scales may be denoted as follows:

$$\frac{dx}{dt} = f(x,y), \quad x \in R^n,\ y \in R^m \tag{2a}$$

$$\frac{dy}{dt} = \epsilon g(x,y), \quad \epsilon \ll 1 \tag{2b}$$

Equation (2b) is called a slow subsystem since the value of y changes slowly while eq.(2a) a fast subsystem. The

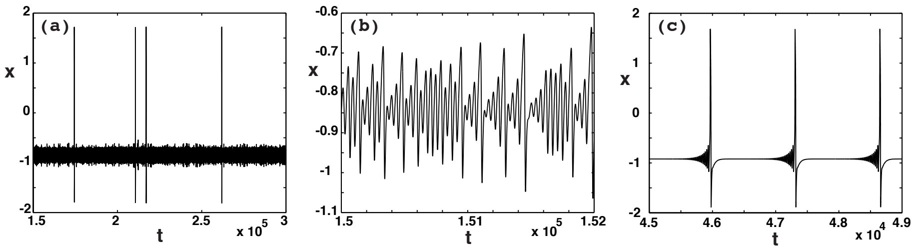

Figure 2: Example of slow spiking in the BVP equations. **(a)** $a = 3.0$, $b = 1.0$, $\eta = 0.13$, $\epsilon = 0.01$, $I_{\text{ext}} = -0.477175$. **(b)** Magnification of the lower-left part of (a). **(c)** $a = 1.5$, $b = 1.0$, $\eta = 0.1$, $\epsilon = 0.01$, $I_{\text{ext}} = -0.874$.

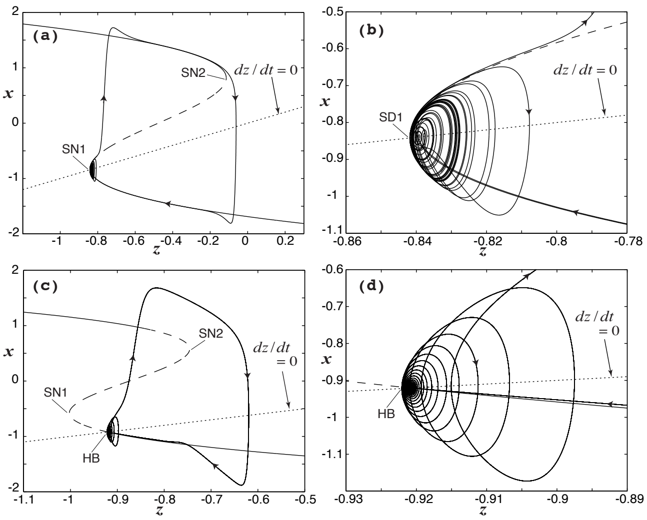

Figure 3: Slow-fast decomposition analysis of the BVP equations. **(a,b)** Parameter values are the same as Fig.2(a). **(c,d)** Parameter values are the same as Fig.2(c).

whole equations (2) are called a full system especially. So-called slow-fast analysis divides the full system to the slow and fast subsystems. In the fast subsystem (2a), the slow variable y is considered as a constant or a parameter. The variable x changes more quickly than y and thus x is considered to stay close to the attractor (stable equilibrium points, limit cycles, etc.) of the fast subsystem for a fixed value of y. The variable y changes slowly with a velocity $\epsilon g(x, y)$ in which x is considered to be in the neighborhood of the attractor. The attractor of the fast subsystem may change if y is varied. The problem of analysis of the dependence of the attractor on the parameter y is a bifurcation problem. Thus the slow-fast analysis reduces the analysis of the full system to the bifurcation problem of the fast subsystem with a slowly-varying bifurcation parameter. In the case of the BVP equations (1), the corresponding slow subsystem is eq.(1c) and the remaining equations (1a,b) are the fast subsystem.

Figure 3 shows the slow-fast decomposition analysis of the BVP equations. Panel (a) corresponds to the case of Fig.2(a). The Z-shaped curve denotes the equilibrium points of the fast subsystem (1a,b) of the BVP equations as a function of the slow variable z in which solid and broken curves denote stable and unstable equilibrium points, respectively. The stability of equilibrium points of the fast subsystem changes by the saddle-node bifurcations SN1 and SN2. The dotted line is the z-nullcline $dz/dt = 0$. The solution curve (with arrow symbols) of the full system of the BVP equations is also superimposed. It is seen that the solution of the full system switches between the upper and lower branches of Z-shaped curve near the saddle-node bifurcation points SN1 and SN2 of the fast subsystem. The upper branch corresponds to a generation of spike and, before the spike generation, the solutions stays near SN1 for a long time which corresponds to a sub-threshold (chaotic) oscillation. Panel (b) is the magnification of the neighborhood of SN1 of (a) from which the solution is considered to be a chaotic solution. Figure 3(c) shows the slow-fast analysis which corresponds to the solution of Fig.2(c). Differently from Fig.3(a) the solution of the full system leaves the lower branch at the neighborhood of the Hopf bifurcation point HB of the fast subsystem. Panel (d) is the magnification of the departure or the switching point HB which shows that this solution is a periodic orbit.

As is seen from Fig.3, the switching (which corresponds to a spike generation) from the lower branch of the equilibrium curve of the fast subsystem occurs in two different ways: One is at the saddle-node bifurcation point and the other at the Hopf bifurcation point of the fast subsystem. In the former case, the sub-threshold (chaotic) oscillation is the main part of the long ISI and in the latter case, a longtime stay near the unstable equilibrium point of the full system is the main part of the long ISI. This dependency of the two different mechanisms of long ISI generation on the switching types is same as the case of the HH equations [3].

4. Hopf Bifurcation in Singularly Perturbed Systems

Let us examine the difference of bifurcations of the fast subsystem more quantitatively. Let x^* denote the equilibrium point of the BVP equations (1). Then the Jacobian matrix at the equilibrium point is

$$\begin{pmatrix} 1 - x^{*2} & -1 & -1 \\ \eta & -\eta a & 0 \\ \epsilon & 0 & -\epsilon b \end{pmatrix} \tag{3}$$

The condition so that this matrix could possess a pair of pure imaginary eigenvalues (the necessary condition for the

Hopf bifurcation of the *full* system) is obtained as:

$$(\eta a + x^{*2} - 1)\eta\{1 + a(x^{*2} - 1)\} = O(\epsilon) \quad (4a)$$
$$\omega^2 \equiv \eta\{1 + a(x^{*2} - 1)\} > 0 \quad (4b)$$

where we assumed that $\epsilon \ll 1$. On the other hand, the characteristic equation of the *fast* subsystem is

$$\lambda^2 + (\eta a + x^{*2} - 1)\lambda + \eta\{1 + a(x^{*2} - 1)\} = 0 \quad (5)$$

The condition (4a) corresponds to the two cases: (i) $(\eta a + x^{*2} - 1) = O(\epsilon)$ or (ii) $1 + a(x^{*2} - 1) = O(\epsilon)$. As is seen from eq.(5), in the singular limit of $\epsilon = 0$, the case (i) and (ii) correspond to the Hopf and the saddle-node bifurcations of the *fast* subsystem, respectively. In the case (ii) (the switching occurs at the saddle-node bifurcation of the fast subsystem), the full system possesses a pair of pure imaginary eigenvalues $\pm i\omega$ at the Hopf bifurcation point of the *full* system where $\omega = O(\sqrt{\epsilon})$. Thus, the period of the periodic orbit *immediately after* the Hopf bifurcation *of the full system* becomes large as ϵ decreases. (Note that the long ISIs shown in Fig.1 are much longer than this period.) On the other hand, in the case (i), the period does not depend on ϵ much since $\omega^2 \equiv \eta\{1 + a(x^{*2} - 1)\}$ is not so small in this case.

Let us denote the eigenvalues of the matrix (3) by α and $\mu \pm i\omega$. The real eigenvalue α at the Hopf bifurcation of the full system is $-(\eta a + x^{*2} - 1) + O(\epsilon)$. In the case (ii) that the switching occurs at the saddle-node point of the fast subsystem, if there exists a Silnikov-type homoclinic orbit near the Hopf bifurcation of the full system, then an inequality $|\alpha/\mu| > 1$ holds since μ becomes small near the Hopf bifurcation of the full system. Thus, in the case (ii), if there is such a homoclinic orbit, then chaotic behavior will appear near the homoclinic orbit by the Silnikov's theory. This is consistent with our simulation result of Fig.1(a-i)-(a-iii), although the existence of such a homoclinic orbit is not yet confirmed. On the other hand, in the case (i), the relation between $|\alpha|$ and μ is not clear since $|\alpha| = |\eta a + x^{*2} - 1|$ is also small. In order to clarify this relation, the more elaborate analysis which incorporates the higher-order terms of ϵ is necessary.

5. Discussion

We have shown that chaotic and very slow oscillation can appear near a Hopf bifurcation of an equilibrium point using the three-dimensional BVP equations. This phenomenon is unexpected and interesting since the Hopf bifurcation is very local one while both the chaotic and slow oscillations are global phenomena. It appears that this phenomenon occurs in a generic way in singularly perturbed systems, although the precise condition for the occurrence are still under our investigation. Especially, the consideration on the similarity and dissimilarity between the smooth BVP equations considered here and the piecewise-linearized BVP equations [4] may help for this problem. The relevance, *if any*, to the so-called canards in R^3 is also an interesting future subject [12, 13, 14].

References

[1] S. Doi, J. Inoue and S. Kumagai, "Chaotic spiking in the Hodgkin-Huxley nerve model with slow inactivation of the sodium current," *J. Integrative Neurosci.* 3, 207-225, 2004.

[2] S. Doi and S. Kumagai, "Slow-fast analysis of bifurcations in a multi-dimensional Bonhoeffer-van der Pol neuronal model," *Proc. NOLTA 1997*, 193-1196, 1997.

[3] S. Doi and S. Kumagai, "Nonlinear dynamics of small-scale biophysical neural networks," In: R. Poznanski (ed.) *Biophysical Neural Networks: Foundations of Integrative Neuroscience*, Chapter 10, 261-301, Mary Ann Liebert, Inc, 2001.

[4] S. Doi and S. Kumagai, "Complicated slow oscillations with simple switching dynamics in a piecewise linear neuronal model," *Proc. 47th IEEE International Midwest Symposium on Circuits and Systems*, pp.II-609–II-612, 2004.

[5] J. Drover, J. Rubin, J. Su and B. Ermentrout, "Analysis of canard mechanism by which excitatory synaptic coupling can synchronize neurons at low firing rate," *SIAM J. Appl. Math.*, accepted.

[6] R. FitzHugh, "Impulses and physiological states in theoretical models of nerve membrane," *Biophy. J.* 1, 445-466, 1961.

[7] J. Guckenheimer, "Towards a global theory of singularly perturbed dynamical systems," *Prog. Nonl. Diff. Eq. Appl.* 19, 213-225, 1996.

[8] J. Guckenheimer, R. Harris-Warrick, J. Peck and A. Willms, "Bifurcation, bursting, and spike frequency adaptation," *J. Comp. Neurosci.* 4, 257-277, 1997.

[9] J. Guckenheimer and A. Oliva, "Chaos in the Hodgkin-Huxley model," *SIAM J. Appl. Dynam. Sys.* 1, 105-114, 2002.

[10] J. Guckenheimer and A. R. Willms, "Asymptotic analysis of subcritical Hopf-homoclinic bifurcation," *Physica D* 139, 195-216, 2000.

[11] J. Honerkamp, G. Mutschler and R. Seitz, "Coupling of a slow and a fast oscillator can generate bursting," *Bull. Math. Biol.* 47, 1-21, 1985.

[12] N. Kakiuchi and K. Tchizawa, "On an explicit duck solution and delay in the Fitzhugh-Nagumo equation," *J. Diff. Eq.* 141, 327-339, 1997.

[13] K. Tchizawa, "On ducks in the minimal system with codimension two," *Dynamics of Continuous Discrete and Impulsive Systems-Series B-Applications & Algorithms* 10, 363-375, 2003.

[14] M. Wechselberger, "Existence and bifurcation of canards in R^3 in the case of a folded node," *Tech. Rep. 13, Math. Biosci. Inst., Ohio State Univ.*, 2003.